Evidence for large configuration-induced band-gap fluctuations in $GaAs_{1-x}N_x$ alloys

G. Bentoumi, V. Timoshevskii, N. Madini, M. Côté, and R. Leonelli*
Département de Physique and Regroupement Québécois sur les Matériaux de Pointe (RQMP), Université de Montréal, Case Postale 6128, Succursale Centre-ville, Montréal, Québec H3C 3J7, Canada

J.-N. Beaudry, P. Desjardins, and R. A. Masut
Département de Génie Physique and Regroupement Québécois sur les Matériaux de Pointe (RQMP), École Polytechnique, Case Postale 6079, Succursale Centre-ville, Montréal, Québec H3C 3A7, Canada
(Received 3 March 2004; published 23 July 2004)

We have measured the near-band-gap absorption of $GaAs_{1-x}N_x$ thin films with $x<0.012$. The spectra were analyzed with a model which allows a precise determination of the band gap and of the width of the optical transitions; the latter is found to increase, for $x>0.002$, well beyond what is expected in a III-V alloy. *Ab initio* calculations were performed within the generalized-gradient approximation with the exchange-correlation functional of Engel and Vosko [Phys. Rev. B **47**, 13164 (1993)]. They reveal that the band gap depends markedly on nitrogen atomic configuration. The anomalous broadening of the intrinsic optical transitions thus gives strong evidence for configuration-induced band-gap fluctuations.

DOI: 10.1103/PhysRevB.70.035315 PACS number(s): 78.20.Ci, 71.15.−m, 71.20.Nr, 78.66.Fd

I. INTRODUCTION

Because of the high electronegativity and small size of nitrogen, a partial replacement of arsenic with nitrogen has profound effects on the electronic structure of GaAs.[1,2] One of the most striking properties of GaAsN alloys is a dramatic reduction of the fundamental band gap.[3–6] This behavior can be reproduced by the band anticrossing (BAC) model[7–9] which postulates that nitrogen generates resonant localized states above the conduction band (CB) of GaAs. These dispersionless states interact with the extended states of the CB, giving rise to two nonparabolic subbands E_- and E_+ with energies

$$E_{\pm}=\frac{1}{2}\{[E_0+E_N]\pm\sqrt{[E_0-E_N]^2+4xC^2}\}, \quad (1)$$

where E_0 is the energy of the GaAs CB, E_N is the bare average energy of the nitrogen-induced states and C is the hybridization matrix element. Equation (1) accounts well for the composition dependence of the band gap of GaAsN alloys with $E_N=1.65$ eV and $C=2.7$ eV at 300 K (Ref. 2) and it can be incorporated in a tight-binding scheme to predict the energy levels of GaAsN-based heterostructures.[10] However, there still exists significant scatter between different data sets or even within a given set as most of the reported data were obtained using low-resolution absorption or modulated reflectance techniques performed at temperatures above 80 K.

A somewhat different picture emerges from first-principles calculations performed within the local density approximation (LDA)[11–14] as well as empirical pseudopotential (EP) calculations.[1,15–17] It is found that the strong N-induced perturbation of the host crystal mixes the Γ_{1c}, L_{1c}, and X_{1c} states and thus modifies the electronic properties of the alloy with respect to GaAs. EP calculations also reveal the strength and anisotropy of N-N interactions which generates localized cluster states below the conduction band in the ultradilute limit.[17] These states partially control the low-temperature emission properties of $GaAsN_{1-x}N_x$ samples[4,18–21] but their impact on the intrinsic electronic properties of this unusual semiconductor in the alloy regime is still a subject of debate.

Photoluminescence (PL) gives information on the optical quality of semiconductors but low-temperature, near band gap absorption experiments are better suited to provide a deeper understanding of their intrinsic properties. This is because PL is very sensitive to extrinsic states created in the band gap by impurities or defects and to the localized cluster states mentioned above while the absorption coefficient is directly coupled to the band gap joint density of states. We present in this paper high-resolution, low temperature absorption spectra obtained from $GaAs_{1-x}N_x$ thin films with $0.0004<x<0.012$. The spectra were quantitatively analyzed with a model which includes electron-hole correlations. We find that the band edge broadens, for $x>0.002$, beyond what is expected for a III-V alloy. This result is correlated to *ab initio* calculations which reveal that the anisotropic N-N interactions play an important role in the band-gap shift down to a nitrogen content as low as 0.01.

II. EXPERIMENTS

Pseudomorphic $GaAs_{1-x}N_x$ thin films in the concentration range $0.0004<x<0.012$ were grown by low-pressure metalorganic vapor phase epitaxy on (001) oriented semi-insulating GaAs substrates. Trimethylgallium, tertiarybutylarsine, and dimethylhydrazine were used as the gas sources of Ga, As, and N, respectively. A 60 nm-thick GaAs buffer layer was first grown on the substrate at 650°C, followed by a 200 nm-thick GaAsN epilayer grown at either 550°C or 600°C. Further details on the growth procedure can be found in Ref. 22. The composition and uniformity of the epilayers were assessed with quantitative secondary ion mass spectroscopy and the lattice parameter measured by high-resolution x-ray diffraction. For all samples in our concentration range, the layers were fully strained and their lattice parameters

 ©2004 The American Physical Society

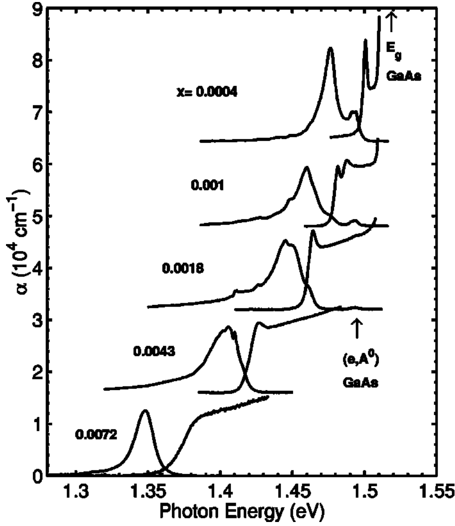

FIG. 1. Absorption coefficient α and PL spectra of $GaAs_{1-x}N_x$ samples for different values of x. The spectra have been shifted for clarity and the PL intensities have been normalized. The arrows indicate the energy position of the band-gap and electron-acceptor transition (e,A^0) in GaAs.

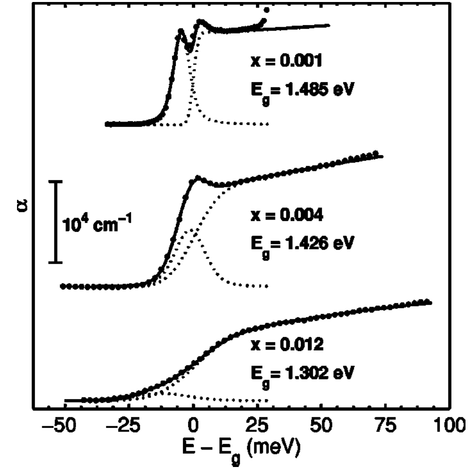

FIG. 2. Absorption coefficient (data points) of $GaAs_{1-x}N_x$ as a function of $(E-E_g)$ for three different concentrations x. The solid lines are fits to the data using Eq. (4). The dotted lines correspond to the exciton and the continuum components of the absorption edge.

varied according to elasticity theory and Vegard's rule. The absorption experiments were performed with the samples mounted strain free in a helium flow cryostat and cooled to 8 K. The spectra were acquired using a Fourier transform spectrometer with a resolution better than 0.5 meV. PL spectra were also acquired using the same setup. The PL was excited with a He-Ne laser at a power density of 250 mW cm^{-2}.

The absorption coefficients for several samples are shown in Fig. 1. An excitonic resonance which gradually broadens with x can be observed up to $x \sim 0.007$, where it can no longer be distinguished from the absorption edge. As previously reported,[18,20] the band-gap shift to lower energy is already present in the sample with the lowest concentration x. The near-gap PL spectra of the samples is also shown in Fig. 1. The main feature in the PL spectra is an emission band with full width at half maximum (FWHM) ranging from 10 to 25 meV. We attribute this emission to band-to-neutral acceptor $(e,A)^0$ transitions, although emission from excitons trapped in near-edge localized states cannot be excluded for the samples with high nitrogen content.

III. DISCUSSION

In order to extract quantitative information from the absorption spectra, electron-hole correlations must be taken into account. The strength of these correlations is controlled by the exciton binding energy $R^* = \mu e^4/(32\pi^2\epsilon^2\hbar^2)$, where μ is the exciton reduced mass and ϵ the permittivity. For direct transitions between nondegenerate parabolic bands, the absorption coefficient $\alpha(\hbar\omega)$ takes the form[23]

$$\alpha = \frac{C}{\hbar\omega}\left[2R^* F_1(\hbar\omega - E_X) + \int_{E_g}^{\infty} \frac{F_2(\hbar\omega - E)}{1 - e^{-2\pi/\sqrt{z}}} dE\right], \quad (2)$$

where only the dominant 1s exciton state has been included. In Eq. (2), $z=(E-E_g)/R^*$, $E_X=E_g-R^*$, C is a constant which depends on the interband transition matrix elements, and F_1 and F_2 are line shape functions with unit surfaces. In binary III-V semiconductors, the main broadening mechanism at low temperature originates from impurity scattering and Eq. (2) reproduces well the observed near-gap absorption coefficient with Lorentzian line shapes.[24] In ternary alloys, compositional disorder on a microscopic scale also broadens the transitions. For a zinc-blende random alloy, the broadening is well described by a Gaussian with a full width at half-maximum (FWHM) Γ_G given by[25]

$$\Gamma_G = 2\sqrt{2\ln 2}\left[\frac{3}{16\pi}\left(\frac{a_0}{a_B}\right)^3 x(1-x)\right]^{1/2}\left|\frac{\partial E_g}{\partial x}\right|, \quad (3)$$

where $a_B=e^2/(8\pi\epsilon R^*)$ is the exciton Bohr radius and a_0 is the lattice constant.

Equation (2) does not fully apply to GaAsN layers on GaAs(001) because the difference in lattice parameters gives rise to a tensile strain which lifts the degeneracy at the Γ point between the heavy-hole (hh) and light-hole (lh) valence bands. Using elasticity theory and materials parameters linearly interpolated between those of GaAs and cubic GaN,[26] the energy shifts of the valence subbands can be evaluated as $\delta E_{lh} \simeq 2.6x$ eV and $\delta E_{hh} \simeq 1.0x$ eV. The effect of a biaxial strain is however not limited to subband splitting: the strain also mixes the $hh|\frac{3}{2},\frac{3}{2}\rangle$ and $lh|\frac{3}{2},\frac{1}{2}\rangle$ states which acquire anisotropic effective masses.[27] Nevertheless, in GaAs(001) with biaxial tensile strain, the ratio of the oscillator stengths of the lh and hh transitions remains close to the 1:3 ratio of the spin multiplicities.[28]

It follows that the absorption coefficient of our samples should be modeled with Eq. (2) using two different sets of parameters to independently reproduce the lh and hh transitions. However, since the spectra plotted in Fig. 2 do not show any evidence of lh-hh splitting, a simplified fitting function is more appropriate:

TABLE I. Values of the parameters used to fit the absorption coefficients with Eq. (4). Γ_{XL} was maintained fixed at 3 meV for all samples.

x	E_X (eV)	Γ_{XG} (meV)	E_g (eV)	Γ_G (meV)	R^* (meV)	$\delta E_{lh}-\delta E_{hh}$ (meV)
0.0004	1.501	<2	1.505[a]			0.7
0.0010	1.482	4	1.486	3.1	>4	1.5
0.0018	1.464	5	1.466	6.8	1.6	2.9
0.0019	1.462	9	1.466	9.9	1.8	3.0
0.0043	1.425	10	1.426	15	2.3	6.9
0.0072	1.374	25	1.376	16	1.4	12
0.0119	1.292	18	1.302	21	1.6	19

[a]Obtained by setting $R^*=4.2$ meV (Ref. 24).

$$\alpha = \frac{1}{\hbar\omega}\left[A_1 V(\hbar\omega - E_X) + A_2 \int_{E_g}^{\infty} \frac{G(\hbar\omega - E)}{1 - e^{-2\pi z}} dE\right], \quad (4)$$

where A_1 and A_2 are constants, V is a Voigt function with Lorentzian and Gaussian FWHM Γ_{XL} and Γ_{XG} centered at an energy E_X, and G is a Gaussian lineshape with FWHM Γ_G. As shown in Fig. 2, Eq. (4) gives excellent fits to the experimental data with the optimized parameters listed in Table I. Because of the proximity of the GaAs epilayer absorption, no information on the continuum edge could be extracted for the sample with $x=0.0004$. Its exciton resonance was fitted with a Lorenztian contribution $\Gamma_{XL}=3.0$ meV. This value for Γ_{XL} was fixed for the other samples with no loss in the quality of the fits. R^* is determined by the inverse of the slope of the continuum edge above E_g. Since Eq. (4) does not take into account band nonparabolicity, the values of R^* are approximative.[29] In contrast, the values of E_g and Γ_G are determined with a good degree of precision since they depend on the position and extent of the continuum edge transition.

Figure 3 shows the band-gap shift $\Delta E_g=E_g(0)-E_g(x)$. Even though the values are close to those calculated from the BAC model [Eq. (1)], we observe that, for $x>0.002$, the data

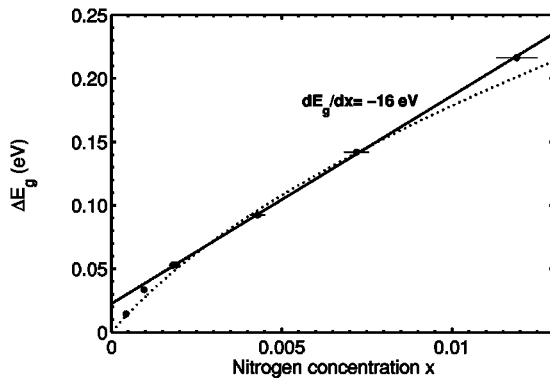

FIG. 3. Experimental band-gap shift $\Delta E_g=E_g(0)-E_g(x)$ as a function of nitrogen concentration x. The solid line is a linear fit to the data points for $x>0.0018$ and the dashed line corresponds to the BAC model [Eq. (1)].

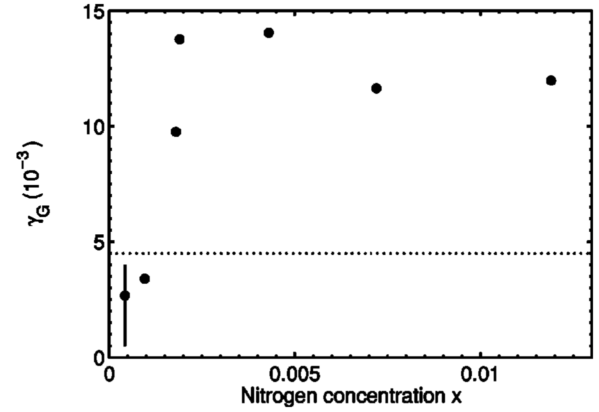

FIG. 4. Normalized gaussian broadening γ_G as a function of nitrogen concentration x. The point at $x=0.0004$ is an estimate obtained from Γ_{XG}. The dashed line gives γ_G obtained from Eq. (5) with a value for a_B equal to that of GaAs.

points are linearly distributed with a slope $\partial E_g/\partial x=-16$ eV. For $x<0.001$, ΔE_g deviates from the linear dependence as the data points converge towards $\Delta E_g=0$ for $x=0$. A similar trend at very low nitrogen content has been recently reported by Taliercio *et al.* (Ref. 6).

Further information can be obtained from the values of Γ_G. First, these values are larger than the expected *lh-hh* splitting. Given the 1:3 ratio of the respective oscillator strengths, this explains why the *lh* and *hh* transitions cannot be resolved in our spectra. In order to follow variations in materials characteristics as a function of nitrogen content, it is best to introduce a normalized Gaussian broadening,

$$\gamma_G = \frac{\Gamma_G}{\sqrt{x(1-x)}}\left|\frac{\partial E_g}{\partial x}\right|^{-1} = \sqrt{\frac{3\ln 2}{2\pi}}\left(\frac{a_0}{a_B}\right)^{3/2}. \quad (5)$$

The data points in Fig. 4 show γ_G for our samples. In dilute conventional III-V alloys, γ_G is nearly constant. Its value in the limit $x\to 0$, which can be evaluated using Eq. (5) with $\epsilon=12.5\ \epsilon_0$ and $R^*=4.2$ meV,[24,26] is depicted as a dashed line in Fig. 4. As can be seen, the experimental values are close to the expected one for the samples with $x\leqslant 0.001$, but a sharp threefold increase occurs at $x\sim 0.002$.

Assuming the validity of Eq. (5) for the full composition range of our samples, the exciton reduced mass μ can be evaluated from the definition of the Bohr radius a_B. We find $\mu\simeq 0.04\ m_0$ for the sample with $x=0.001$ and $\mu\simeq 0.09\ m_0$ for the samples with a larger nitrogen content, where m_0 is the free electron mass. The former value is close to that of pure GaAs $(0.05\ m_0)$ while the latter agrees well with a value of $0.1\ m_0$ in an InGaAsN sample with 1% nitrogen, deducted from PL linewidth measurements.[30] The related change in CB effective mass cannot however be easily deducted from the PL linewidth broadening since, as pointed out by Senger and Bajaj (Ref. 31), the exact nature of the radiative centers is not known. On the other hand, the same hole contributions to the exciton reduced mass as in GaAs is expected for the conduction to valence-band transitions involved in absorption measurements. The rise of γ_G at $x\sim 0.002$ would then imply an abrupt fourfold increase of m_e^*, a very unlikely sce-

TABLE II. Calculated band-gap shifts and effective masses in ordered GaAsN.

x	Supercell size and lattice	E_g (eV)	m_e^* EV-GGA	BAC	$m_{hh}^{\Gamma X}$	$m_{lh}^{\Gamma X}$
0		1.17	0.068	0.067	0.34	0.083
0.0093	216-sc	0.92	0.088	0.096	0.34	0.083
0.0156	128-fcc	0.73	0.097	0.101	0.34	0.083
0.0313	64-sc	0.69	0.087	0.109	0.34	0.082
0.0370	54-fcc	0.30	0.077	0.110	0.35	0.062

nario! A significant departure from full randomness could also enhance the broadening but there is yet no evidence for such a departure at a low nitrogen content.[32] The validity of Eq. (5) must thus be questioned as another broadening mechanism than compositional fluctuations is probably involved.

In an attempt to identify this mechanism, we have undertaken *ab initio* band-structure calculations within the density functional theory (DFT) approach. We started with the ABINIT code,[33] which uses the planewave pseudopotential method within the local density approximation for the exchange-correlation (XC) functional. Full geometry optimization was performed for a simple GaAs structure as well as for four supercells with different lattices and nitrogen contents, as described in Table II. We then refined our calculations by using the generalized gradient approximation with the XC functional proposed by Engel and Vosko[34] (EV-GGA) to obtain the electronic properties of the LDA-relaxed structures. These calculations were performed with the WIEN2K code which is a full-potential linearized augmented planewave method and therefore has the further advantage of not using pseudopotentials. The EV-GGA functional improves significantly the values of the band gap for GaAsN: the 54-atom system remains a semiconductor when its band gap is calculated with the EV-GGA while it is already metallic within the LDA. Furthermore, the EV-GGA gives an electron effective band mass close to the experimental one[35] while it is several times too small when calculated within the LDA.[14] We also included spin-orbit coupling which allows the determination of the light-hole masses.

The main results of the calculations are summarized in Table II and Fig. 5. As expected, the calculated effective masses of pure GaAs are close to the experimental values. As the N content increases, the valence band masses are left unchanged except for the supercell with the highest nitrogen content while the CB effective mass increases according to the predictions of the BAC model[8] up to $x=0.016$ and then decreases. The decrease at high nitrogen content may be due to the fact that the calculated band gaps are lower than the experimental ones, resulting in stronger interactions between conduction and valence bands. Nevertheless, our calculations show that the band masses do not change sufficiently to account for the observed increase of γ_G at $x\sim 0.002$.

As for the band-gap shift ΔE_g, it not only depends on x but also on supercell lattice: ΔE_g is significantly higher when the nitrogen atoms are ordered along the $\langle 110\rangle$ directions (fcc lattice) than along the $\langle 100\rangle$ directions (sc lattice). Anisotropic N-N interactions have already been previously reported for very low concentrations[13,17] and for nitrogen chains at very short distances.[16] Our *ab initio* calculations further reveal that they also play an important role in the band-gap shift of ordered GaAsN. In a disordered alloy, configuration variations which inevitably occur on a scale of the order of the exciton Bohr radius will induce band-gap fluctuations which must be added to those induced by composition fluctuations. Anisotropic N-N interactions thus constitute a mechanism which can explain the observed anomalous broadening of the optical transitions. The sharp rise of γ_G which happens at $x\sim 0.002$ can then be interpreted as a transition from isolated to interacting nitrogen atoms.

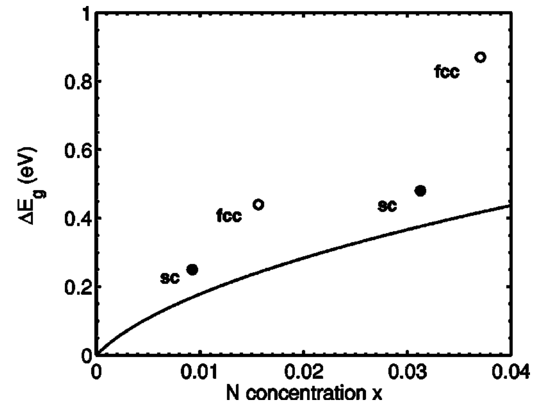

FIG. 5. Calculated band-gap shift $\Delta E_g = E_g(0) - E_g(x)$ as a function of nitrogen concentration x. The solid line corresponds to the BAC model [Eq. (1)].

IV. CONCLUSIONS

In conclusion, an in-depth analysis of the low-temperature absorption spectra of $GaAs_{1-x}N_x$ samples indicate that, for $x>0.002$, the near band-gap intrinsic transitions are much broader than expected for a conventional III-V alloy. In parallel, *ab initio* calculations performed with up to 216-atom supercells show that the GaAsN band gap strongly depends on the supercell lattice. Even though the calculations describe ordered crystals, they reveal that strong nitrogen-nitrogen interactions still occur in structures with a nitrogen content as low as 1%. We thus conclude that large configuration-induced band-gap fluctuations generate the observed anomalous broadening. These results highlight new important properties of GaAsN compounds which are not taken into account by macroscopic descriptions such as the band anticrossing model.

ACKNOWLEDGMENTS

We are indebted to S. Guillon for the SIMS measurements. This work was supported by the Natural Sciences and Engineering Research Council of Canada (NSERC) and by the Fonds Québécois de la Recherche sur la Nature et les Technologies (FQRNT). The computational resources were provided by the Réseau Québécois de Calcul de Haute Performance (RQCHP).

*Electronic address: richard.leonelli@umontreal.ca

[1] P. R. C. Kent and A. Zunger, Phys. Rev. B **64**, 115208 (2001), and references contained therein.

[2] I. Vurgaftman and J. R. Meyer, J. Appl. Phys. **94**, 3675 (2003), and references contained therein.

[3] J. Toivonen, T. Hakkarainen, M. Sopanen, and H. Lipsanen, J. Cryst. Growth **221**, 456 (2000).

[4] P. J. Klar, H. Grüning, W. Heimbrodt, J. Koch, W. Stolz, P. M. A. Vicente, and J. Camassel, Appl. Phys. Lett. **76**, 3439 (2000).

[5] R. Chtourou, F. Bousbih, S. B. Bouzid, F. Charfi, J. C. Harmand, G. Ungaro, and L. Largeau, Appl. Phys. Lett. **80**, 2075 (2002).

[6] T. Taliercio, R. Intartaglia, B. Gil, P. Lefebvre, T. Bretagnon, U. Tisch, E. Finkman, J. Salzman, M.-A. Pinault, M. Laugt *et al.*, Phys. Rev. B **69**, 073303 (2004).

[7] W. Shan, W. Walukiewicz, J. W. Ager, III, E. E. Haller, J. F. Geisz, D. J. Friedman, J. M. Olson, and S. R. Kurtz, Phys. Rev. Lett. **82**, 1221 (1999).

[8] C. Skierbiszewski, P. Perlin, P. Wisniewski, T. Suski, J. F. Geisz, K. Hingerl, W. Jantsch, D. E. Mars, and W. Walukiewicz, Phys. Rev. B **65**, 035207 (2001).

[9] J. Wu, W. Shan, and W. Walukiewicz, Semicond. Sci. Technol. **17**, 860 (2002).

[10] N. Shtinkov, P. Desjardins, and R. A. Masut, Phys. Rev. B **67**, 081202 (2003).

[11] E. D. Jones, N. A. Modine, A. A. Allerman, S. R. Kurtz, A. F. Wright, S. T. Tozer, and X. Wei, Phys. Rev. B **60**, 4430 (1999).

[12] N. Gonzalez Szwacki and P. Boguslawski, Phys. Rev. B **64**, 161201 (2001).

[13] L.-W. Wang, Appl. Phys. Lett. **78**, 1565 (2001).

[14] I. Gorczyca, C. Skierbiszewski, T. Suski, N. E. Christensen, and A. Svane, Phys. Rev. B **66**, 081106 (2002).

[15] T. Mattila, S.-H. Wei, and A. Zunger, Phys. Rev. B **60**, R11245 (1999).

[16] A. Al-Yacoub and L. Bellaiche, Phys. Rev. B **62**, 10847 (2000).

[17] P. R. C. Kent and A. Zunger, Phys. Rev. Lett. **86**, 2613 (2001).

[18] T. Makimoto, H. Saito, T. Nishida, and N. Kobayashi, Appl. Phys. Lett. **70**, 2984 (1997).

[19] S. Francoeur, S. A. Nikishin, C. Jin, Y. Qiu, and H. Temkin, Appl. Phys. Lett. **75**, 1538 (1999).

[20] H. Grüning, L. Chen, T. Hartmann, P. Klar, W. Heimbrodt, F. Höhnsdorf, J. Koch, and W. Stolz, Phys. Status Solidi B **215**, 39 (1999).

[21] Y. Zhang, A. Mascarenhas, J. F. Geisz, H. P. Xin, and C. W. Tu, Phys. Rev. B **63**, 085205 (2001).

[22] J.-N. Beaudry, R. A. Masut, P. Desjardins, P. Wei, M. Chicoine, G. Bentoumi, R. Leonelli, F. Schiettekatte, and S. Guillon, J. Vac. Sci. Technol. A **22**, 771 (2004).

[23] F. Bassani and G. Pastori Parravicini, *Electronic States and Optical Transitions in Solids* (Pergamon, New York, 1975).

[24] A. R. Goñi, A. Cantarero, K. Syassen, and M. Cardona, Phys. Rev. B **41**, 10111 (1990).

[25] E. F. Schubert, E. O. Göbel, Y. Horikoshi, K. Ploog, and H. J. Queisser, Phys. Rev. B **30**, 813 (1984).

[26] I. Vurgaftman, J. R. Meyer, and L. R. Ram-Mohan, J. Appl. Phys. **89**, 5815 (2001).

[27] G. L. Bir and G. E. Pikus, *Symmetry and Strain-Induced Effects in Semiconductors* (Wiley, New York, 1974).

[28] A. Freundlich, H. Kamada, G. Neu, and B. Gil, Phys. Rev. B **40**, 1652 (1989).

[29] Band nonparabolocity increases the density of state, and thus the absorption coefficient, as the energy increases. Since this enhances the slope of the continuum edge, the values of R^* obtained from Eq. (2) underestimate the actual exciton binding energy, as found in Ref. 24.

[30] E. D. Jones, A. A. Allerman, S. R. Kurtz, N. A. Modine, K. K. Bajaj, S. T. Tozer, and X. Wei, Phys. Rev. B **62**, 7144 (2000).

[31] R. T. Senger and K. K. Bajaj, J. Appl. Phys. **94**, 7505 (2003).

[32] H. A. McKay, R. M. Feenstra, T. Schmidtling, and U. W. Pohl, Appl. Phys. Lett. **78**, 82 (2001).

[33] X. Gonze, J.-M. Beuken, R. Caracas, F. Detraux, M. Fuchs, G.-M. Rignanese, L. Sindic, M. Verstraete, G. Zerah, F. Jollet *et al.*, Comput. Mater. Sci. **25**, 478 (2002).

[34] E. Engel and S. H. Vosko, Phys. Rev. B **47**, 13164 (1993).

[35] C. Persson, R. Ahuja, and B. Johansson, Phys. Rev. B **64**, 033201 (2001).